20th International Conference on Renewable Energies and Power Quality (ICREPQ'22)
Vigo (Spain), 27th to 29th July 2022
Renewable Energy and Power Quality Journal (RE&PQJ)
ISSN 2172-038 X, Volume No.20, September 2022

Contribution of a photovoltaic solar system to the energetic sustainability of a Portuguese WWTP

Bruno Eira[1,2], Paulo Pinto[2], Joaquim Carneiro[1]

[1] Centre of Physics of Minho and Porto Universities (CF-UM-UP), Gualtar Campus, University of Minho, 4710-057 Braga, Portugal
brunoeira22@gmail.com, carneiro@fisica.uminho.pt
[2]MEGAJOULE S.A.
Trav. Honório de Lima, 16; 4465-171 S. Mamede Infesta (Portugal)
paulo.pinto@megajoule.pt

Abstract. The concerning growth of energy and water demand worldwide presents two major issues that can both be tackled by using renewable energy sources to oppose the energy consumption of wastewater treatment plants (WWTP), while taking advantage of their energy production potentialities. This work deals with the sizing of a photovoltaic system of a medium-sized Portuguese WWTP designed to meet the energy consumption needs, benefitting from the higher levels of irradiance in the country. The goal is to act as a model for future similar projects. The potentiality of producing electricity through cogeneration of biogas, in WWTP's of activated sludge, needs to be taken into account. In the study case, 70% of the energy consumption needs were covered via cogeneration. This led to the conception of two different scenarios concerning the PV System: the first one covers the total electric needs of the WWTP and the other covers 30%, taking into account that the cogeneration system ensures 70%. During the 25 year-life of the PV System, an average annual performance ratio of 0.805 for scenario 1 and 0.789 for scenario 2 was achieved. Furthermore, the average energy contribution of scenario 1 and 2 was 36.5% and 32.8%, respectively, ensuring 100% of self-sufficiency, when adding the cogeneration contribution.

Keywords. Photovoltaic, WWTP, Energy efficiency, Self-sufficiency, Renewable energies

1. Introduction

The global energy demand suffered a 4% reduction from 2019 to 2020, a value that was influenced by the global pandemic crisis associated with the SARS Cov-2 disease, as well as the CO_2 emissions that in April 2020 registered a daily average decrease of 26 % . However, these values represent an atypical variation, with an increase of 6% in energy demand registered in 2021 (the steepest since 2010) [1]. In the more realistic scenarios, this growth is expected to continue in the coming years [1], relating to the projected population increase, which points to a growth of about 22% of the total world population by 2050. In order to suppress this tendency, a proportional increase in energy availability will continually be needed, creating a higher pressure over fossil fuels. The goal established by the International Renewable Energy Agency (IRENA) aims to sustain the global energy demand from renewable energy sources (RES), projecting for 2050 a representatively of 2 thirds of all energy. In recent years, RES growth has been enhanced in European Union especially due to the fast growth and expansion of wind and solar photovoltaic (PV) energy [1]. Despite accounting for only 2.8% of all world electricity production, solar PV has experienced the sharpest increase among all RES in 2019, recording a remarkable growth of 24.3% worldwide, with Africa (96.7%) and the Middle East (95.4%) being the regions of the globe that have registered a more significant percentage increase.

In recent years, the investment in solar PV energy was evident, recording the worldwide all-time highest increase in production (32%), from 2019 to 2020, with a total of 821 000 GWh of electric energy being produced in that year [1]. This tendency is followed in Portugal, where there is a huge potential for the installation of solar PV panels, due to the geo-climatic favourable conditions, associated with irradiance levels above the European average.

Beyond energy resources, the industrial activity has caused an excessive use of other types of resources. Recent predictions based on factors such as demographic growth and the increase of pollution in terrestrial subsystems, point towards an increase in water demand for the domestic sector, as well as for industry and agriculture, ranging from 20% to 30%, until 2050. Due to the growing limitations of natural resources, the interaction water-energy assumes a very important value, not just because the water treatment requires electricity, but also because they interconnect in the consumption of other products.

Therefore, an implementation of a large-scale model that consists of increasing Portuguese WWTPs' energetic self-sufficiency, by supplying its intensive energy needs with photovoltaic grid connected energy production systems should be carried out to mitigate the high demand for both water and energy.

2. WWTP Energetic Balance

A. Energy Consumption Pattern

To ensure that a preliminary assessment of the WWTP's energy consumption outlook was assembled, two years of energy consumption data (2019 and 2020) from the Paço de Sousa WWTP were taken into account, as well as the energy produced via the biogas cogeneration system. The energy data (kWh) had an hourly resolution. The data was also divided between different treatment stages, being possible to arrange it into groups of consumers, providing relevant information on which groups hold the largest energetic slice and where to focus on a future energy efficiency study. Figure 1 shows the share of energy consumption distributed by those consumer groups.

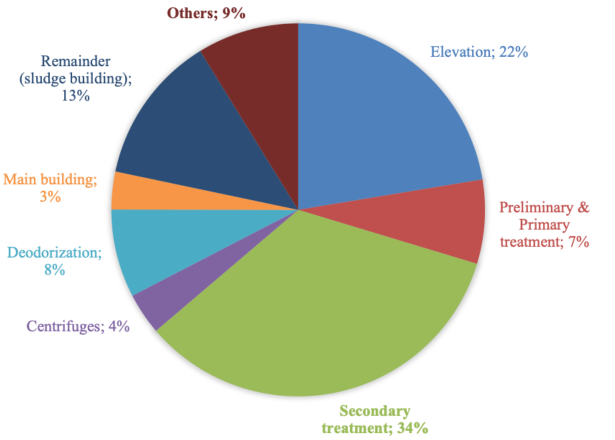

Fig. 1 Paço de Sousa's WTTP energy consumption share of each of the largest consumer groups.

To evaluate the seasonality of the energy consumption on the two-year data, a yearly average load diagram was developed, as shown in Table I. Annually the Paço de Sousa WWTP consumes an average of 1,503 GWh of electric energy.

Table I - Average hourly energy consumption for each month of the average year (2019 and 2020).

WWTP average hourly energy consumption (kWh)												
Hour	**Jan**	**Feb**	**Mar**	**Apr**	**May**	**Jun**	**Jul**	**Ago**	**Sep**	**Oct**	**Nov**	**Dec**
0	169	169	179	181	189	188	195	190	195	190	189	165
1	168	166	177	179	185	191	197	191	190	185	187	167
2	166	163	172	173	182	185	193	187	181	181	184	165
3	164	160	169	167	178	175	180	180	176	177	179	160
4	163	156	162	164	168	170	175	170	170	172	174	160
5	160	154	159	158	161	162	167	167	161	165	168	157
6	155	151	155	150	154	151	156	161	156	155	159	155
7	149	146	148	144	148	148	152	151	147	149	152	151
8	149	145	147	144	149	149	153	153	150	145	149	149
9	154	151	149	145	151	152	156	158	161	147	156	148
10	157	153	153	149	155	154	160	164	177	154	159	148
11	159	155	158	153	163	159	169	171	185	159	161	151
12	160	156	161	155	166	165	174	176	189	159	163	149
13	157	158	165	158	169	168	178	184	196	163	168	150
14	158	158	165	160	171	171	186	187	197	168	167	152
15	162	164	169	164	175	176	193	189	200	172	171	151
16	162	165	169	167	182	181	194	195	200	178	178	155
17	167	169	174	171	184	185	200	196	200	181	184	163
18	172	169	174	175	185	187	197	188	195	180	186	165
19	171	171	177	176	185	187	195	188	187	185	186	166
20	169	172	182	177	185	184	194	186	194	184	188	165
21	168	175	180	184	189	187	197	189	199	186	189	167
22	168	175	182	182	186	190	201	189	196	188	190	167
23	167	174	181	180	190	191	199	190	195	190	189	167

The energy demand is significantly higher for the drier months. The daily consumption pattern is similar for each month, showing an increase during the afternoon period, and a decrease during the night, reaching the lowest energy consumption value between 7:00 and 10:00 AM, as evidenced by the daily load profile shown in Figure 2.

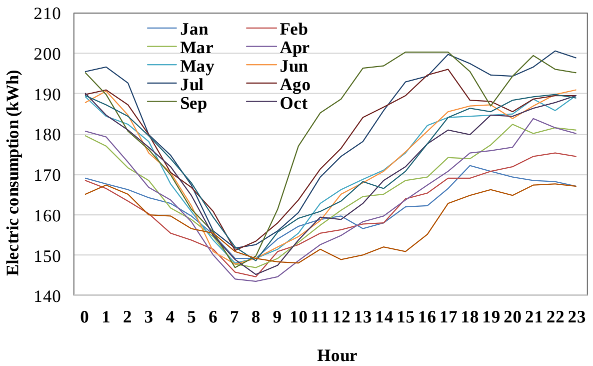

Fig. 2. Daily load profile for each month of the average year (2019 and 2020).

B. Biogas cogeneration system: Energy contribution

Once 2020 was the first full year in which the biogas cogeneration system was operating, it is important to understand the current energy balance of the WWTP. In this way, using the same methodology as before, an attempt was made to draw up an annual production diagram but, unfortunately, during the year 2020, the system had some issues and it did not work fully during the last months of the year.
However, if the atypical period is neglected and energy produced in a month in full operation, such as January, is considered, then it is possible to generate a scenario for the percentage value of energy contribution for a complete year based on monthly consumption data. This scenario is shown in Table II.

Table II - Daily energy contribution of the cogeneration system, in a fully operational scenario, per month.

	Daily energy consumption [kWh]	**Daily production (fully working scenario) [%]**
January	3893.82	82.92%
February	3875.27	83.32%
March	4004.83	80.62%
April	3953.81	81.66%
May	4148.49	77.83%
June	4154.31	77.72%
July	4361.39	74.03%
August	4301.23	75.07%
September	4399.98	73.38%
October	4111.91	78.52%
November	4176.55	77.31%
December	3793.59	85.11%
Average	4097.93	78.79%

Nonetheless, this data couldn't be considered for further analysis since it does not account for periods related with maintenance or other periodic events that will reduce the energy production's feasibility. Considering this fact, an energy contribution of 70% by the aforementioned system was considered.

3. Sizing of PV System

A. Site geography and area availability

To suppress, or mitigate as much as possible, the WWTP's energy needs and ensure that there was a neutral or positive energy balance, the installation of a production unit under a self-consumption regime, with connection to the grid for sale of instant energy production, without the use of battery storage was proposed.

In this sense, two scenarios were proposed for the installation of the photovoltaic solar plant since the efficiency in the production of biogas was an important issue to be considered.

The first scenario was designed for peak consumption, completely disregarding the energy produced by cogeneration, with the sale of extra energy to the grid.

In the second scenario, the PV plant was designed to offset the negative balance between the average energy production produced by cogeneration (under favourable conditions) and the peak consumption of the WWTP.

The entire solar plant sizing methodology, for both scenarios, was performed using the PVsyst software [2], but an assessment of the available land at the WWTP was previously carried out, selecting the exact location for the implementation of the PV system.

Figure 3 is an aerial view of the Paço de Sousa WWTP, where the available area (A_{av}) of 3192 m^2 is marked in red. This place is located at an altitude of 151 m above sea level.

As mentioned before, the design of the photovoltaic system was carried out using the commercial PVsyst software, which is a computer code dedicated to the study, design and data analysis of complete PV systems. PVsyst enables the user to obtain and interpolate meteorological data (from the station or using satellite imagery), but also other databases, such as PV modules, inverters, regulators, generators, and pumps, as well as general calculation tools for solar engineering [2].

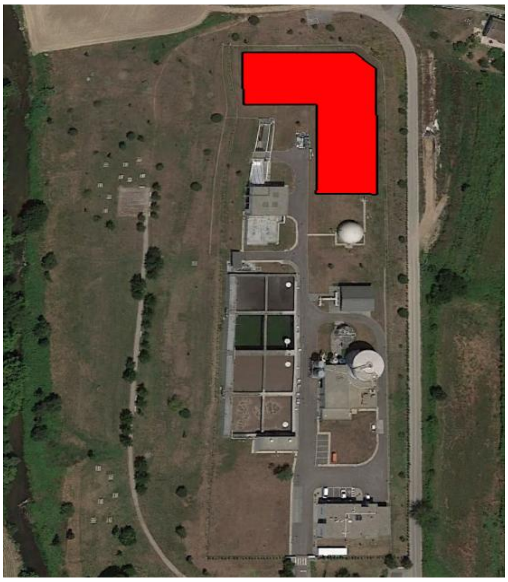

Fig. 3. Aerial view of the WWTP at Paço de Sousa and available area for solar plant installation (*adapted from Google Earth 2021*©).

B. PV plant orientation & meteorological data

Once the location for the installation was decided, the plant orientation was defined. The solar panels will be fixed in a tilted plane. The optimal tilt angle (β_{opt}) was calculated through a normalization of the local latitude ($\emptyset$) [3], using equation (1), resulting in a optimal tilt angle (β_{opt}) of 32,11°.

$$\boldsymbol{\beta_{opt} = 3.7 + 0.69\emptyset} \quad (1)$$

The azimuth (α) represents the angle of deviation in relation to the south direction, and in this case study it was taken as α = 0°, orienting the panels towards south.

The monthly horizontal global radiation is the amount of energy that irradiates over a unit of area, during a month (Wh/m²/month). To obtain data about solar radiation, solarimetric instruments are normally used, such as the pyranometer [3] which allows to obtain the power values on a flat surface (Irradiance, G (W/m^2)); however the PVsyst software allows for an alternative model to obtain the irradiation data.

The global horizontal irradiation (I_{global}) of the installation site was extracted from a database integrated in PVsyst: Meteonorm. This meteorological database includes weather data for solar engineering applications. It aggregates measurements of the nearest meteorological stations, interpolating the data from a 3D inverse distance modelling of the weather stations to the intended location.

In this case study, 10-year time series (1996-2005) were provided by Meteonorm. If the closest station is located more than 10 km from the location, satellite data are used simultaneously, to help and increase the accuracy of the obtained values [4].

The hourly horizontal global irradiation data were interpolated from the four closest stations. As the closest station is located at a distance greater than 10 km from the location, 62% of the data were covered via satellite.

In addition to the irradiation data, Meteonorm also provided average daily values for temperature, relative humidity, and precipitation, as shown in Table III.

Table III. - Monthly meteorological parameters for a typical meteorological year (TMY): global horizontal irradiation (I_{global}), horizontal diffuse irradiation ($I_{diffuse}$), temperature (T), relative humidity (HR) and precipitation (PP).

Month	I_{global} [kWh/m²]	$I_{diffuse}$ [kWh/m²]	T [°C]	HR [%]	PP [mm]
Jan	56.5	24.0	9.7	81.6	137
Feb	79.2	36.8	10.2	77.8	75
Mar	121.7	51.0	12.2	74.3	119
Apr	156.7	71.9	13.7	76.7	106
May	199.0	76.9	16.1	74.9	61
Jun	210.3	74.0	18.3	76.8	30
Jul	219.7	70.1	19.6	77.4	23
Aug	194.7	68.0	20.0	75.6	32
Sep	148.6	52.5	18.7	77.2	58
Oct	95.8	41.8	16.8	77.9	144
Nov	62.8	29.7	12.5	80.3	148
Dec	48.0	20.6	10.6	79.8	168

C. PV installed power methodology

The methodology used for scenario 1 consisted of sizing the PV system to suppress the month that required more power to satisfy its energetic needs (critical month). However, as the available area limits the plant, it may not be possible to fulfil the energetic needs. Therefore, the following criteria was applied:

i. Sizing to fulfil the energetic needs for the critical month
ii. Sizing to fulfil the energetic needs for the month with higher energetic needs
iii. Sizing to fulfil the energetic needs for the month with more irradiation
iv. Sizing to fill the available area

The same criteria was followed in scenario 2, except that, for this scenario, the energy needs were calculated based solely on 30% of the energy consumption, since we're considering the contribution given by the biogas cogeneration system.

To address the power needed to suppress the monthly needs, some calculations were made. Firstly, the average daily solar equivalent hour (H_S) for each month was determined. This value represents the time period equivalent to the daily solar irradiation corresponding to the peak power (for STC conditions, where G = 1000 W/m^2) [3].

$$H_{S_{\text{daily}}} = \frac{I(\beta_{opt})}{1000} \quad (2)$$

Power to be installed (P_{PV}) was defined as the total power that is necessary to be installed to cover energy needs (L), considering the number of equivalent solar hours (H_S) each month and the inevitable losses of the system. In this calculation, two power reduction factors are considered, namely R_1, which corresponds to the losses of the PV module and R_2 is the losses due to cabling. Preliminary values of 0.9 for R_1 and 0.75 for R_2 were considered.

$$P_{PV} = \frac{(L_{\text{critical month}})}{H_s R_1 R_2} \quad (3)$$

The installed power based on covering the energetic needs for each month was calculated for scenario 1 and scenario 2, as shown in Table IV and Table V.

Table IV. –Values obtained for required power (P_{FV}) based on the average energetic daily needs for each month of the year.

Month	Daily energy consumption [kWh/day]	Daily solar equivalent hours (Hs)	Energetic needs (L) [kWh/day]	Required power (P_{FV}) [kWp]
Jan	3893,82	1,82	3953,11	3212,36
Feb	3875,27	2,83	3934,29	2060,02
Mar	4004,83	3,93	4065,82	1533,88
Apr	3953,81	5,22	4014,02	1138,16
May	4148,49	6,42	4211,66	971,70
Jun	4154,31	7,01	4217,58	891,08
Jul	4361,39	7,09	4427,81	925,32
Aug	4301,23	6,28	4366,73	1029,73
Sep	4399,98	4,95	4466,98	1335,64
Oct	4111,91	3,09	4174,53	2000,67
Nov	4176,55	2,09	4240,15	2999,95
Dec	3793,59	1,55	3851,36	3683,89

Table V. -Values obtained for required power (P_{FV}) to suppress 30% of the energy needs for each month of the year.

Month	Energetic needs (L) [kWh/day]	Daily solar equivalent hours (H_S)	Required power (P_{FV}) [kWp]
Jan	1081,97	1,82	879,22
Feb	1076,81	2,83	563,83
Mar	1112,81	3,93	419,82
Apr	1098,64	5,22	311,51
May	1152,73	6,42	265,96
Jun	1154,35	7,01	243,89
Jul	1211,89	7,09	253,26
Aug	1195,17	6,28	281,84
Sep	1222,61	4,95	365,56
Oct	1142,57	3,09	547,58
Nov	1160,53	2,09	821,09
Dec	1054,12	1,55	1008,28

Based on the obtained monthly values for scenario 1 and considering the limitation of 1MW due to the Portuguese legislation, the 4th criteria was chosen, and the only option was to cover the area as efficiently and logical as possible. The second scenario was limited by the 2nd criteria, and the planned power was equivalent to fulfil 30% of the month with more energetic needs: September.

1) PV module and inverter

The selected PV module model was Jinko Solar's JKM580M-7RL4-V. This PV module has a peak power output (for STC conditions) of 580 Wp.

In the present study, 125 kW three-phase inverters were selected, since higher power inverters point to values in the MW range and do not adjust to the installed power in the PV plant. The inverter selection was based on the planned power, ensuring there was a ratio close to 1:1 between the power of the PV system (P_{FV}) and the power of the inverter (P_{INV}).

The selected inverter model was the Sungrow SG125HV.

2) Scenario 1: Sizing methodology

Initially, the area available for installation was divided into three parts, because of the different widths (see Figure 4). The size of the rows and the number of PV modules connected in series (N_S), in addition to the limits established by the electrical specifications of the PV module and the inverter, were also determined by the width of these three areas.

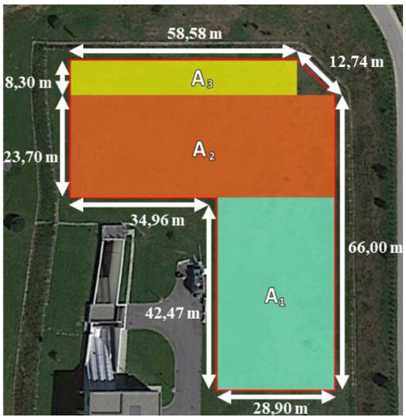

Fig.4. Division of the available area in three distinct areas.

Considering area A1, the width (W-E) of 28.90 m must be fully used by the PV panels, without being exceeded, complying the intervals determined by the voltage and current intensity characteristics of the modules and the inverter.

Initially, the maximum number of PV modules connected in series (N_S) supported by the inverter was calculated from the ratio between its maximum voltage ($V_{max\ INV}$) and the PV module voltage for the lowest temperature ($V_{CA\ (T=-10\ °C)}$). The maximum calculated limit was 25 modules per string.

The minimum value was also calculated, accounting for the input voltage of the inverter ($V_{min\ INV}$) and the module voltage for the highest temperature ($V_{mp\ (T\ =\ 60\ °C)}$). The obtained minimum limit was 22 modules per string.

The JKM580M-7RL4-V module is 2.411 m long and 1.134 m wide, thus being possible to assemble it horizontally or vertically.

Considering the modules arranged horizontally, the minimum possible value for the width of the PV panels can be calculated from the module length and the minimum value of modules connected in series (N_S = 22). Since the width of the PV panel significantly exceeds the width of area A1, the modules were arranged vertically.

The ideal width of the PV panels for N_S = [22, 23, 24, 25] was calculated, to determine the closest value to the smallest width of the three areas (area A1: W_{A1} = 28.90 m). The number of modules connected in series was 25, as it is the value that better fills the available width, as they occupy 28.39 m of the 28.90 m available (already considering the frame of the modules). In accordance with these calculations, all the PV panels considered for this PV system will have strings of 25 modules.

The length of the area occupied by the panels was then calculated. For this calculation, the considered variables were the number of strings per PV panel (N_F) and the pitch N-S, which accounts for the space between consecutive PV panels to avoid self-shading. The pitch was calculated based on the trigonometric relation between the solar height angle (Υ), the optimum tilt angle (β) and the width of the PV panel. Obviously, the length of the pitch increases proportionally to the number of strings of the panels.

In order to determine the number of strings per PV panel of a given area k (N_{FAk}), an interval of N_{FAk} = [1, 2, 3, 4, 5] was considered.

The maximum length occupation of each area was calculated for each value.

In the present methodology, two criteria were followed to ensure the better layout design:

- Selecting the value that provides the highest power.
- The exceeded length by one area shall not limit the northernmost area.

The same rules were applied to area A2; however, for this area, it was possible to place two PV panels side by side. Regarding area A3, as it is the northernmost area of the PV plant, the only concern was to ensure that the area length was not exceeded. In this case, the pitch was not relevant because no more panels were susceptible of being shaded.

Following this methodology, the layout of scenario 1 was elaborated as shown schematically in Figure 5.

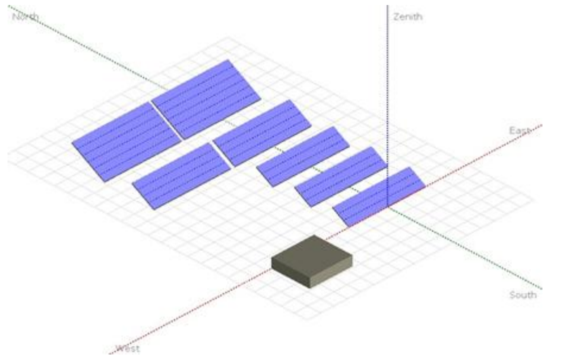

Fig.5. Configuration of the PV solar plant for scenario 1. The closest building is represented in grey (PVsyst).

This layout provides for the installation of 725 modules having a combined power of 420.05 kW. To adjust the power ratio between the PV system and the inverter, three 125 kW inverters were installed in parallel, ensuring a P_{nom} ratio of 1.12.

3) Scenario 2: Sizing methodology

For scenario 2, an identical procedure was followed, but for this case, the objective was to meet the 365 kW. Thus, the construction of the PV system was based on the configuration used in the previous scenario. The difference lies in the PV panels included in area A3, which require fewer strings than in scenario 1, as it brings together two PV panels placed side by side, in which one of them includes four strings of modules and the other has five, as shown in Figure 6.

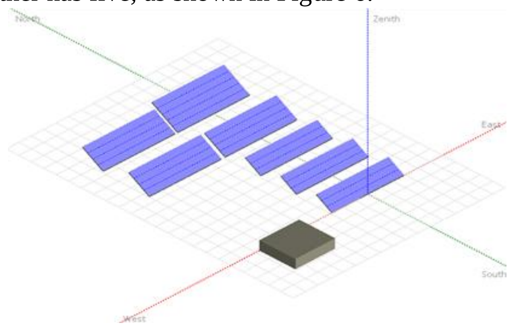

Fig.6. Configuration of the PV plant for scenario 2. The closest building was represented in grey (PVsyst).

An adjustment was also made so the last string was filled with the 25 modules, increasing the installed power from 365 kW to 377 kW.

Just like in scenario 1, the installation of three 125 kW Sungrow inverters was proposed, guaranteeing a P_{nom} ratio of 1.05.

D. Energy production estimate

To assess the energy produced from each scenario, some important detailed losses were considered in PVsyst. While some losses such as annual degradation and LID were specified in the PV module's datasheet, the shading losses (far and near shadings) were calculated by the software based on the defined PV plant configuration. Soiling losses were calculated based on the precipitation hourly data and considering three periods of scheduled cleaning. After accounting for all the losses, a performance ratio (PR) was obtained for both scenarios.

The PR was calculated in both scenarios for each month, averaging a yearly value of 80.5% and 78.9% for scenario 1 and scenario 2, respectively. Based on the monthly gross energy production, which was established by the product of the array's nominal power and the global incident irradiation on the plane, net energy production was calculated, accounting for all system energy losses.

The energy production was seasonal and obviously peaks in July (the month with more irradiance) predicting, in the first year, a peak production of 76.58 MW for scenario 1 (see Figure 7 (a)) and 70.22 MW for scenario 2 (see Figure 7 (b)).

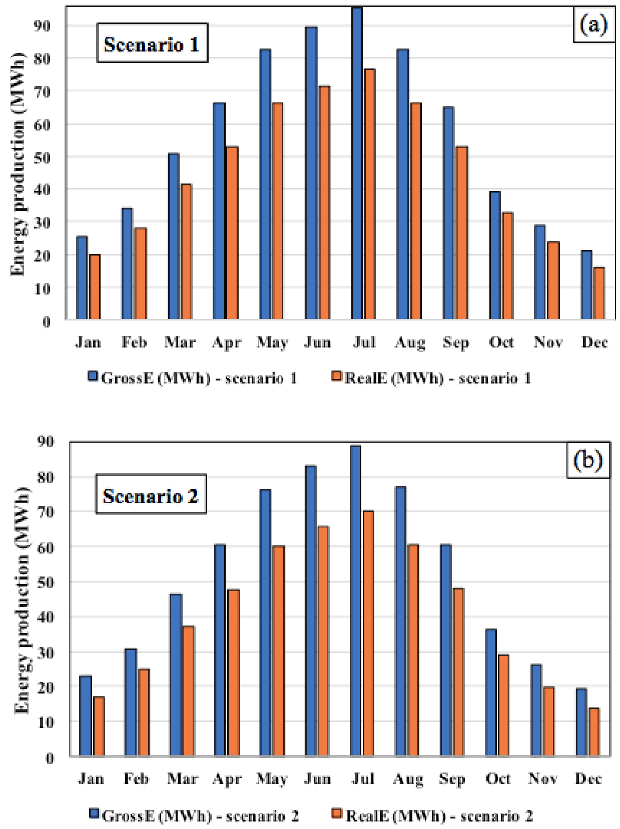

Fig 7. Monthly energy production – PVSyst: (a) scenario1, and (b) scenario 2.

Concerning the first year, the estimated losses for the scenario 1 were not only lower in percentage, as established by the PR, but were also lower in absolute value, as shown on table VI.

Table VI. Energy production estimates and calculated losses

Scenario	Gross production (1st year) (MWh)	Net production (1st year) (MWh)	Average WWTP's yearly consumption (MWh)	Total losses (MWh)
1	681.51	548.23	1503.07	97.28
2	627.04	493.36	1503.07	133.68

E. Energy contribution

The annual energy contribution of the PV system was also calculated for its 25 year-life, considering an annual degradation for the PV modules of 0.55%. Figure 8 plots the change in the energy contribution over the 25-year life of the PV system for the two analysed scenarios.

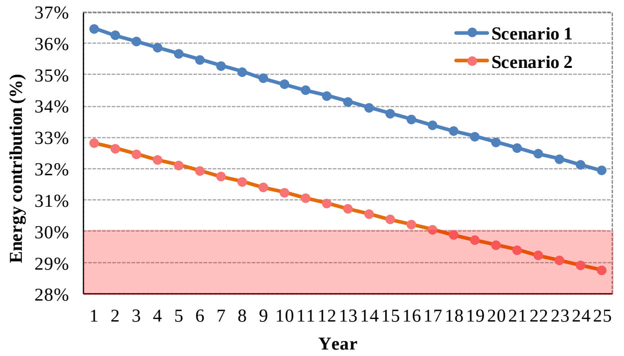

Fig 8. Change in the energy contribution for scenarios 1 and 2 over the 25-year life of the PV system.

4. Conclusion

In scenario 1, the predicted energy contribution was always above 30% throughout the 25-year life of the PV system, which means that if the biogas cogeneration system is fully functional, the WWTP can operate with total energy self-sufficiency for this entire period. In scenario 2, total self-sufficiency is also ensured until the 17th year.

Based solely on energy contribution, the scenario 1 is recommended because of its higher performance ratio, which provides fewer losses, despite having a greater installed power.

Taking scenario 2, it is also possible to achieve total annual self-sufficiency for 25 years, provided that there is a future increase in the efficiency of the WWTP treatment processes, especially secondary treatment. As the energy is not stored, the aforementioned self-sufficiency does not mean that the WWTP consumes all the produced energy, but rather that the yearly energy produced is greater than the consumed one.

To implement this model in a large-scale context, targeting other medium activated sludge Portuguese WWTPs, it is necessary to evaluate the specifics of each case, such as the availability of area for the photovoltaic installation as well as the availability of solar irradiation. Additionally, a consumption analysis must also be performed in order to evaluate each specific treatment procedure.

The synergy between the photovoltaic system and the biogas cogeneration system in activated sludge WWTPs should be encouraged, since it resorts to the use of RES, while enabling a more self-sufficient water treatment.

References

[1] IEA (2022), *Electricity Market Report - January 2022*, IEA, Paris https://www.iea.org/reports/electricity-market-report-january-2022.

[2] PVSyst. PVSyst 7 - Grid Connected, https://www.pvsyst.com/wp-content/uploads/2020/10/PVsyst_Tutorials_V7_Grid_Connected.pdf.

[3] Carneiro J, Passos M. *Sistemas Fotovoltaicos - Fundamentos sobre dimensionamento.* ENGEBOOK, www.quanticaeditora.pt (2020).

[4] Meteonorm. *Handbook part II (7) : Theory Global Meteorological Database Version 7 Software and Data for Engineers , Planers and Education*.